

X-ray absorption spectroscopy at a protein crystallography facility: the Canadian Light Source beamline 08B1-1

Received 28 March 2012
Accepted 22 September 2012Julien J. H. Cotelesage,^{a,b*} Pawel Grochulski,^b Ingrid J. Pickering,^a
Graham N. George^a and Michel N. Fodje^{b*}^aDepartment of Geological Sciences, University of Saskatchewan, 114 Science Place, Saskatoon, SK, Canada S7N 5E2, and ^bCanadian Light Source, 101 Perimeter Road, Saskatoon, SK, Canada S7N 0X4. E-mail: julien.c@usask.ca, michel.fodje@lightsource.ca

It is now possible to perform X-ray absorption spectroscopy (XAS) on metalloprotein crystals at the Canadian Macromolecular Crystallography Facility bend magnet (CMCF-BM) beamline (08B1-1) at the Canadian Light Source. The recent addition of a four-element fluorescence detector allows users to acquire data suitable for X-ray absorption near-edge structure and extended X-ray absorption fine-structure based studies by monitoring fluorescence. CMCF beamline users who wish to supplement their diffraction data with XAS can do so with virtually no additional sample preparation. XAS data collection is integrated with the established *Mx Data Collector* software package used to collect diffraction data. Mainstream XAS data-processing software packages are available for the users; assistance with data processing and interpretation by staff is also available upon request.

© 2012 International Union of Crystallography
Printed in Singapore – all rights reserved**Keywords:** X-ray absorption spectroscopy; XANES; EXAFS; Canadian Light Source; Canadian Macromolecular Crystallography Facility; protein crystallography.

1. Introduction

It has been estimated that metalloproteins constitute between 22 and 30% of the genomic output of most organisms (Waldron & Robinson, 2009; Cotelesage *et al.*, 2012). In particular, metalloenzymes containing transition metal ions are responsible for much of the most challenging chemistry carried out by biological systems. Thus, for a significant number of proteins, bound metal atoms and their immediate atomic environment are a focus of interest for which detailed knowledge is needed in order to understand chemical mechanism. As useful and informative as high-resolution protein crystal structures are, there are often unavoidable impediments that limit what the technique can reveal at the atomic level (Acharya & Lloyd, 2005; Cotelesage *et al.*, 2012). For example, when interpreting crystal structures of metalloproteins, phenomena such as Fourier ringing can complicate interpretation of the region around the metal (Schindelin *et al.*, 1997; Cotelesage *et al.*, 2012). In light of this it is obvious that accurate and high-resolution structural data are critical for researchers in the many fields that study enzyme function and catalysis.

X-ray absorption spectroscopy (XAS) is a technique that can complement protein crystallography. XAS exploits the absorption edge of the element of interest to derive structural information in the vicinity of that element (Strange *et al.*,

2005). Protein crystallographers routinely utilize absorption edges of metalloprotein crystals to obtain initial phase information for solving crystal structures (Matthews, 1966). The XAS of a metalloprotein is acquired by extending the range of measurement above the edge energy. Within about 50 eV of the absorption edge the fine structure of XAS is termed the X-ray absorption near-edge structure (XANES) which provides information on the oxidation state of the metal and some information on the coordination geometry (Cotelesage *et al.*, 2012). Extending to higher energies (400 eV or more) above the absorption edge, the extended X-ray absorption fine structure (EXAFS) can be measured. The EXAFS provides detailed interatomic parameters such as the distance between the metal and its coordinating ligands, often with accuracies of better than ± 0.02 Å, a magnitude better compared with protein crystallography. Collection of adequate signal-to-noise is often an issue with biological samples and typically spectra must be collected multiple times and averaged before structural information can be derived from the data (George & Pickering, 2007).

One of the most significant limitations of XAS is that even under the best experimental conditions only the region around the metal can be probed for structural information. Typical metalloprotein EXAFS will only reveal atomic distances within a 3–4 Å radius of the metal centre (George & Pickering, 2007; Cotelesage *et al.*, 2012), though under certain

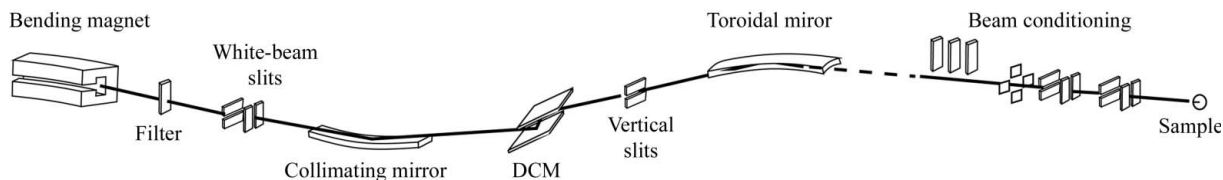


Figure 1
Schematic representation of the Canadian Light Source CMCF-BM (08B1-1) beamline.

circumstances the interpretable EXAFS may extend to longer distances (Cotelesage *et al.*, 2012). Moreover, if the metal of interest binds to multiple sites in the protein, or if exogenous metal is present in the sample solvent, or if the metal binding mode is heterogeneous, it may not be possible to distinguish absorption from the individual metal environments. Despite these limitations XAS has proven to be reliable and in some cases has answered questions that protein crystallography alone has been unable to fully address (George *et al.*, 1999; Yano & Yachandra, 2009; Pushie & George, 2011; Cotelesage *et al.*, 2012).

Measurement of X-ray absorption requires a monochromatic source of radiation with good energy resolution. For each element of interest the radiation must be tunable in small increments from just below the absorption edge to at least a few hundred electronvolts beyond it. Most synchrotron-based macromolecular crystallography beamlines should be able to meet these requirements for most of the biologically relevant metals of the first transition row and above. XAS also requires an appropriate detector to measure absorbance. With concentrated samples, absorbance can be measured by monitoring the incoming and transmitted intensities of radiation. When the concentration of the element of interest is dilute, in the millimolar to micromolar range, a more suitable detection method is to measure the fluorescence of the element of interest as it is proportional to absorbance (Latimer *et al.*, 2005; George & Pickering, 2007; Yano & Yachandra, 2009).

While there are dedicated XAS beamlines at a number of synchrotron facilities, the uncertainty in the utility of XAS may dissuade some protein crystallographers from attempting an experiment. For others, the additional time and resources needed to run on a different beamline may be a barrier to performing XAS on metalloproteins. With some modifications most protein crystallography beamlines that currently collect anomalous edge data could add the capability to measure X-ray absorption on crystal samples. The Canadian Macromolecular Crystallography Facility (CMCF) beamline 08B1-1 now has this capability, allowing users who would otherwise not have the chance to perform XAS-based experiments the opportunity to delve into the field without requiring a significant investment in time or resources.

2. Materials and methods

2.1. Beamline characteristics and requirements

The Canadian Light Source (CLS) beamline 08B1-1 (CMCF-BM) is a bending-magnet-based beamline (Fig. 1)

capable of producing monochromatic radiation from 4000 to 18000 eV (Grochulski *et al.*, 2012). CMCF-BM can be run manually or with a Stanford Auto-Mounter system (Cohen *et al.*, 2002). Data collection is controlled by users with the *Mx Data Collector (MxDC)* software (Fodje *et al.*, 2012) operated either at the CLS or remotely. A four-element Vortex ME4 fluorescence detector (SII NanoTechnology USA Inc., Northridge, CA, USA) has been mounted in a location which does not affect X-ray diffraction data collection. A Soller slit assembly is mounted on the detector to minimize unwanted scatter and fluorescence (Bewer, 2012). Samples are kept at temperatures of 100 K with a cryojet (Oxford Instruments, Abingdon, UK) to minimize radiation damage (Fig. 2) and X-ray induced photochemistry (George *et al.*, 2012).

2.2. Sample preparation for XAS on protein crystals

For successful XAS measurement, any solvent or cryoprotectant around the protein crystal sample should be free from exogenous elements, including the metal of interest, that may interfere with the measurement of fluorescence. Washing the crystal in mother liquor that is free from the elements of concern and then remounting the crystal is normally sufficient to make the sample suitable for XAS. Other than that major caveat, XAS measurements can be performed on a sample already prepared for X-ray diffraction. Users can have their sample run following diffraction data collection. The transi-

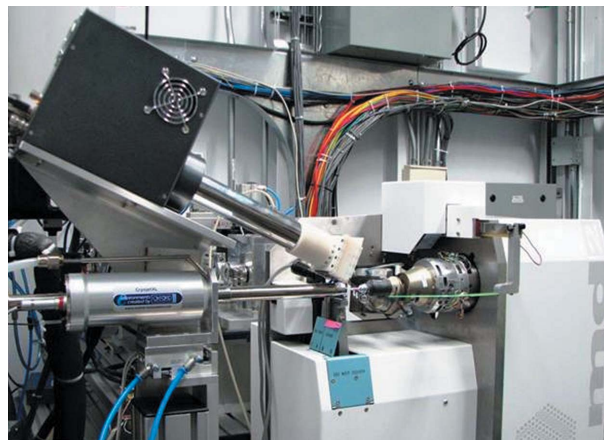


Figure 2
Image of the overall set-up at the CMCF 08B1-1 beamline end-station taken from the perspective of the CCD X-ray detector. The sample is mounted on the goniometer (bottom right) just to the left of the beamstop (green). On the left side of the image is the cryojet (bottom) and Vortex ME4 detector (top). The Soller slit assembly mounted on the front of the detector (white cap) has slots allowing the use of foil filters to reduce unwanted scatter and fluorescence.

tion between diffraction data collection and XAS data collection takes less than 5 min on CMCF-BM.

One other concern for users would be the consequence of lengthy exposure times. Each scan can take from 20 min to an hour. In order to collect enough data to yield results comparable with a dedicated XAS beamline, collection times of up to ten hours per sample may be required. The user must determine whether the exposure times are causing significant radiation damage. Fortunately, relevant radiation damage can be monitored by examining any changes in the XANES on successive sweeps (Yano *et al.*, 2005; George *et al.*, 2012).

2.3. Data collection and processing

The *MxDC* software package used at 08B1-1 for crystallographic data collection has been modified to accommodate XAS data collection. *MxDC* already allowed for control of XANES-based spectroscopy which is normally used for determining the energies required for MAD and SAD crystallographic experiments (Fodje *et al.*, 2012). An additional scan mode has been added specifically for collecting EXAFS data, which contains many of the basic features of other XAS data acquisition programs (*e.g.* George, 2000). The absorbing element of interest, collection time, number of scans and the k -range are selected by the user. The energy above the absorption edge (the EXAFS region) can be scanned as a function of photoelectron wavevector k ,

$$k = [(2m_e/\hbar^2)(E - E_0)]^{1/2}, \quad (1)$$

where all symbols have their usual meanings: m_e is the electron rest mass, E is the X-ray energy, E_0 is the absorption edge threshold energy, and \hbar is Planck's constant divided by 2π . In the EXAFS region the count time per point can vary according to a k -weighting scheme,

$$t = t_{\min} + (t_{\max} - t_{\min})[(k - k_{\min})^n / (k_{\max} - k_{\min})^n], \quad (2)$$

where t is the count time for a given value of k , t_{\min} and t_{\max} are the lower and upper bounds for count-time, respectively, k_{\min} and k_{\max} are the minimum and maximum k , respectively, and n is the power (usually $n = 2$). As is typical on XAS beamlines, a number of individual scans are averaged until data of an acceptable signal-to-noise are obtained.

The output files from each run are saved using the standardized XAS data interchange specification (.xdi file format) to ensure maximal compatibility with XAS software (Newville *et al.*, 2011). Complete log files and raw data from the detectors can be made available at the user's request. Users have access to mainstream XAS data reduction and analysis software such as *ATHENA* (Ravel & Newville, 2005) and *EXAFSPAK* (<http://ssrl.slac.stanford.edu/exafspak.html>). For users with less experience, beamline staff will be available for assistance with processing and interpretation of their collected XAS data.

3. Results

The XAS data from of a small (0.05 mm \times 0.05 mm \times 0.1 mm) protein crystal of *Escherichia coli* phosphoenolpyruvate carboxykinase is shown in Fig. 3. The protein is 540 amino acids in size and has a crystal unit cell containing four manganese (II) atoms (Tari *et al.*, 1997). Owing to the small crystal size no cryoprotectant was used. The crystal's ability to diffract X-rays to ~ 2.0 Å resolution was verified before the XAS analysis was performed. Twelve scans were recorded with each scan taking approximately 50 min to complete. The energy reproducibility of the 08B1-1 monochromator was found to be excellent with a drift of less than 0.1 eV over the total period of data acquisition (almost 10 h). This contrasts with typical protein crystallography data acquisition times which are usually below 2 h for a complete data set. Owing to the small crystal size and the low energy fluorescence of manganese this sample was considered to be at the lower limits of size and atomic number for which satisfactory EXAFS data could be collected at 08B1-1 (Fig. 3).

The data obtained from the runs were processed using *EXAFSPAK* and compared with data collected on equivalent samples at the Stanford Synchrotron Radiation Lightsource (SSRL) dedicated XAS beamline 7-3 using a 30-element Ge

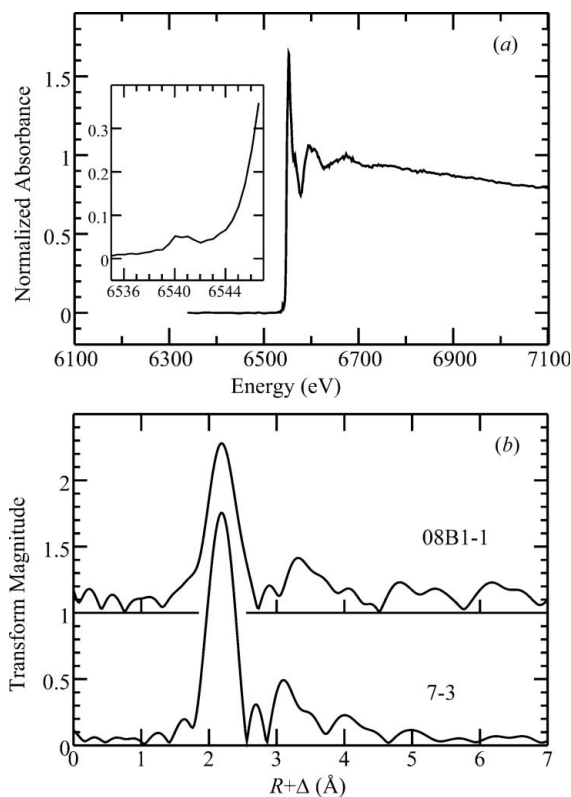


Figure 3 Manganese K -edge X-ray absorption spectroscopy of a crystal of phosphoenolpyruvate carboxykinase from *Escherichia coli*. (a) Normalized background-subtracted spectrum corresponding to the average of 12 individual scans. The inset shows the $1s \rightarrow 3d$ feature expanded to show the detail. (b) Comparison of the Fourier transform of the k^3 -weighted EXAFS obtained from CLS 08B1-1 and SSRL 7-3 calculated using a k -range of $1\text{--}11.5 \text{ \AA}^{-1}$ and phase-correction for Mn–N backscattering.

array detector. The SSRL sample was a large number of crystals suspended in manganese-free mother liquor contained in a standard acrylic sample cuvette with mylar tape windows. Three 35 min sweeps were averaged to give the final data set. Owing to differences in X-ray sources, optics, detectors, cooling temperatures and other factors such as the required sample size, a rigorous comparison between beamlines is beyond the scope of the present work but we note that, while the signal-to-noise from SSRL 7-3 is significantly better than for CLS 08B1-1, the sample volume used at SSRL was approximately 120000 greater. Within this limitation the data collected at 08B1-1 compare well with corresponding data from SSRL 7-3, with reasonable correspondence of the Fourier transforms of the k^3 -weighted EXAFS, but with lower amplitudes for the CLS 08B1-1 data owing to the higher relative sample temperature (100 K at CLS 08B1-1 versus 10 K at SSRL BL7-3). With this example it was possible to collect EXAFS data to a maximum k of approximately 11.5 \AA^{-1} . This data range allows the distinction of atomic distances of about 0.14 \AA (Cotelesage *et al.*, 2012). Higher k -ranges result in improved resolution of similar interatomic distances; the achievable extent of k will depend on the specific experimental conditions, the sample and on the nature of the backscatterers to the metal concerned.

Manganese XAS is often somewhat problematic relative to elements with absorption edges at higher X-ray energies because of X-ray attenuation by windows and flight paths in the experiment. We therefore conducted a second test using a drop of approximately $20 \mu\text{l}$ volume of Zn^{2+} solution contained in a cryo-loop. The sample used was 5 mM Zn^{2+} in the presence of 8 mM reduced glutathione with 30% glycerol as a glassing agent in phosphate buffer at pH 6.9. This sample models the conditions for a large crystal containing reasonably high levels of a metal, and data were acquired over the same time (10 h of averaging) as for the manganese phosphoenolpyruvate carboxykinase discussed above, although in this case the data extended to $k = 14 \text{ \AA}^{-1}$. The data and the EXAFS Fourier transform are of good quality and are shown in Fig. 4.

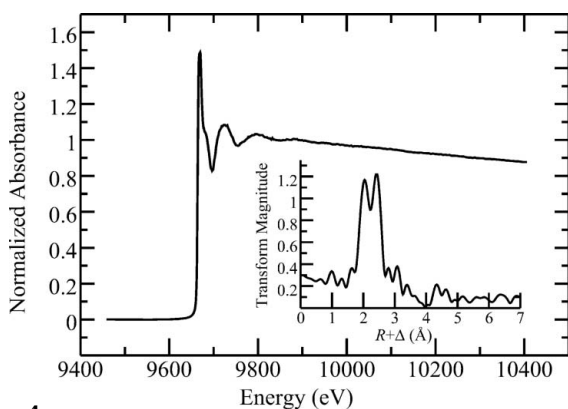


Figure 4
Zinc K -edge X-ray absorption spectroscopy of a $20 \mu\text{l}$ drop of 5 mM Zn^{2+} contained within a crystallographic cryo-loop. The inset shows the EXAFS Fourier transform computed with a k -range of $1\text{--}14.2 \text{ \AA}^{-1}$ and phase-correction for Zn–S backscattering.

4. Discussion and conclusions

CMCF 08B1-1 is designed for protein crystallography and hence has limitations in measuring XAS when compared with dedicated XAS beamlines such as the SSRL beamline 9-3 or the European Synchrotron Radiation Facility (ESRF) beamline FAME. For example, the monochromator at 08B1-1 uses a Si(111) crystal monochromator rather than a Si(220) like the other beamlines, resulting in a diminished range of incident energies. The range for 08B1-1 is 4 to 18 keV compared with 5 to 30 keV for SSRL 9-3 (Latimer *et al.*, 2005) and 4 to 40 keV for ESRF FAME (Proux *et al.*, 2005). Moreover, the energy resolution ($\Delta E/E$) of the monochromator used at 08B1-1 is 1.4×10^{-4} , poorer than the value of 1.0×10^{-4} for SSRL 9-3. This will result in broader features in the XANES spectrum, although the EXAFS should be little affected.

At 08B1-1 samples are cooled with a liquid-nitrogen ‘cryojet’ cryostat (Fig. 2), typically to between 80 and 100 K whereas on XAS beamlines it is often customary to cool to liquid-helium temperatures at around 10 K. The use of a higher sample temperature during data acquisition may render the sample more prone to radiation damage, and also may make it more difficult to resolve some of the finer structural details owing to damping of EXAFS arising from increased thermal contributions to the Debye–Waller factor (*e.g.* Cotelesage *et al.*, 2012). Potentially this could be at least in part remedied by installation of a helium-based ‘cryojet’-type cryostat, with which temperatures of around 20 K can be achieved.

The fluorescence detector currently installed at 08B1-1 has four elements. Larger arrays such as 30-element Ge arrays of discrete detectors or 100-pixel Ge monolith detectors (Canberra Industries, Meriden, CT, USA) are often used on XAS beamlines. The primary reason for the use of such compound devices is that electronic dead-time effects limit the count rate per discrete detector element, and arrays are thus a crude method of operating at overall higher count rates (Cramer *et al.*, 1988). With the present four-element array on 08B1-1, samples may need to be exposed for longer to achieve the equivalent signal-to-noise relative to XAS beamlines with larger detector arrays. This may raise concerns about sample integrity or availability of beam time. Recently, Chantler *et al.* (2012) have reported that self-absorption of a sample contributed to significant variance in the intensity of fluorescence measurements made at each detector element owing to the varied distances the fluorescence has to travel through sample and air. In situations such as this it is beneficial to have redundant measurements from each discrete element making it easier to identify and mitigate the effects of some forms of systemic error (Chantler *et al.*, 2012). While this is a concern for concentrated samples, it is not expected to be a serious problem for XAS-based work on protein crystals because of the dilute nature and small size of the samples. If the density of a protein crystal is taken as 1.22 g cm^{-3} (Andersson & Hovmöller, 2000), assuming a protein molecular weight of 50000 Da and a 1:1 ratio of metal to protein, then the metal concentration is about 20 mM . For samples with metal

concentrations in this range, self-absorption will be significant for larger samples but the small sample sizes for protein crystals (>0.2 mm pathlength) means that these effects will likely not compromise an XAS-based experiment (e.g. Tröger *et al.*, 1992). As far as detectors are concerned, while longer data collection times and lack of access to advanced statistical tools may remain an issue for the time being, there are no limitations at 08B1-1 preventing the addition of a larger multi-element fluorescence detector array in the future.

Despite these challenges, XAS data collected at 08B1-1 can be of great utility for protein crystallographers. The data collected have demonstrated that the recent modifications and additions to the beamline equipment allows the determination of valuable structural information related to the metalloprotein crystal samples already mounted for X-ray diffraction. Properties such as bond distances, oxidization state and geometry can be used to supplement crystallographic data. Beamline 08B1-1 can examine the *K*-shell absorption edges of manganese through zirconium ($Z = 25$ to 40) as well as the *L*-shell absorption edges of elements 57 to 88. Some of the biologically relevant elements in the obtainable ranges include iron, copper, zinc, arsenic, mercury and lead.

For users with little or no experience with XAS the upgrades on 08B1-1 provide an excellent opportunity to explore this new direction. Assistance from CMCF staff is available by request. Users thus face little risk or any major commitments of time and resources if they choose to delve into the field of XAS.

We thank Hughes Goldie (Department of Microbiology, University of Saskatchewan) for providing protein samples. JJHC is a Fellow in the CIHR Training grant in Health Research Using Synchrotron Techniques (CIHR-THRUST). IJP and GNG are Canada Research Chairs and are supported by the Natural Sciences and Engineering Research Council (NSERC) Canada, the Canadian Institutes of Health Research (CIHR) and the Saskatchewan Health Research Foundation. The Canadian Light Source is supported by the NSERC Canada, the National Research Council Canada, the CIHR, the Province of Saskatchewan, Western Economic Diversification Canada, and the University of Saskatchewan.

References

- Acharya, K. R. & Lloyd, M. D. (2005). *Trends Pharmacol. Sci.* **26**, 10–14.
- Andersson, K. M. & Hovmöller, S. (2000). *Acta Cryst.* **D56**, 789–790.
- Bewer, B. (2012). *J. Synchrotron Rad.* **19**, 185–190.
- Chantler, C. T., Rae, N. A., Islam, M. T., Best, S. P., Yeo, J., Smale, L. F., Hester, J., Mohammadi, N. & Wang, F. (2012). *J. Synchrotron Rad.* **19**, 145–158.
- Cohen, A. E., Ellis, P. J., Miller, M. D., Deacon, A. M. & Phizackerley, R. P. (2002). *J. Appl. Cryst.* **35**, 720–726.
- Cotelesage, J. J. H., Pushie, M. J., Grochulski, P., Pickering, I. J. & George, G. N. (2012). *J. Inorg. Biochem.* **115**, 127–137.
- Cramer, S. P., Tench, O., Yocum, M. & George, G. N. (1988). *Nucl. Instrum. Methods Phys. Res. A*, **266**, 586–591.
- Fodje, M., Janzen, K., Berg, R., Black, G., Labiuk, S., Gorin, J. & Grochulski, P. (2012). *J. Synchrotron Rad.* **19**, 274–280.
- George, G. N., Hilton, J., Temple, C., Prince, R. C. & Rajagopalan, K. V. (1999). *J. Am. Chem. Soc.* **121**, 1256–1266.
- George, G. N. & Pickering, I. J. (2007). *Brilliant Light in Life and Material Science*, edited by Vasilii Tsakanov and Helmut Wiedemann, pp. 97–119. Berlin: Springer.
- George, G. N., Pickering, I. J., Pushie, M. J., Nienaber, K., Hackett, M. J., Ascone, I., Hedman, B., Hodgson, K. O., Aitken, J. B., Levina, A., Glover, C. & Lay, P. A. (2012). *J. Synchrotron Rad.* **19**, 875–886.
- George, M. J. (2000). *J. Synchrotron Rad.* **7**, 283–286.
- Grochulski, P., Fodje, M., Labiuk, S., Gorin, J., Janzen, K. & Berg, R. (2012). *J. Struct. Funct. Genom.* **13**, 49–55.
- Latimer, M. J., Ito, K., McPhillips, S. E. & Hedman, B. (2005). *J. Synchrotron Rad.* **12**, 23–27.
- Matthews, B. W. (1966). *Acta Cryst.* **20**, 230–239.
- Newville, M., Ravel, B., Solé, V. A. & Wellenreuther, G. (2011). *Xdispec*, <https://github.com/XraySpectroscopy/XAS-Data-Interchange/wiki/Xdispec>.
- Proux, O., Biquard, X., Lahera, E., Menthonnex, J.-J., Prat, A., Ulrich, O., Soldo, Y., Trévisson, P., Kapoujyan, G., Perroux, G., Tainier, P., Grand, D., Jeantet, P., Deleglise, M., Roux, J.-P. & Hazemann, J.-L. (2005). *Phys. Scr.* **T115**, 970–973.
- Pushie, M. J. & George, G. N. (2011). *Coord. Chem. Rev.* **255**, 1055–1084.
- Ravel, B. & Newville, M. (2005). *J. Synchrotron Rad.* **12**, 537–541.
- Schindelin, H., Kisker, C. & Rees, D. C. (1997). *J. Biol. Inorg. Chem.* **2**, 773–781.
- Strange, R. W., Ellis, M. & Hasnain, S. S. (2005). *Coord. Chem. Rev.* **249**, 197–208.
- Tari, L. W., Matte, A., Goldie, H. & Delbaere, L. T. (1997). *Nat. Struct. Biol.* **4**, 990–994.
- Tröger, L., Arvanitis, D., Baberschke, K., Michaelis, H., Grimm, U. & Zschech, E. (1992). *Phys. Rev. B*, **46**, 3283–3289.
- Waldron, K. J. & Robinson, N. J. (2009). *Nat. Rev. Microbiol.* **6**, 25–35.
- Yano, J., Kern, J., Irrgang, K. D., Latimer, M. J., Bergmann, U., Glatzel, P., Pushkar, Y., Biesiadka, J., Loll, B., Sauer, K., Messinger, J., Zouni, A. & Yachandra, V. K. (2005). *Proc. Natl Acad. Sci.* **102**, 12047–12052.
- Yano, J. & Yachandra, V. K. (2009). *Photosynth. Res.* **102**, 241–254.